Electronic Supplementary Information (ESI†)

The effect of an alkyl chain tether on the kinetics and mechanistic behaviour on bifunctional dinuclear platinum(II) complexes bearing *N,N'*-dipyridylamine ligands

Panyako Wangoli. Asman[a]*and Grace Kinunda[b]

[a]*School of Chemistry and Physics University of KwaZulu-Natal, 3209, Scottsville, Pietermaritzburg, South Africa*

[b]*Chemistry Department, University of Dar es Salaam, P. O. Box 35061, Dar es Salaam, Tanzania.*

E-mail: pwangoli@yahoo.com

A summary of wavelengths used for kinetic measurements for the investigated complexes, some of their kinetic traces, k_{obs} for reactions at different concentrations and temperatures and characterization of complexes using ^{1}H NMR, TOF ES^{+} mass spectra, ^{13}C NMR and ^{195}Pt' NMR are given in the following tables.

Table S1: Summary of the wavelengths used for monitoring kinetic reactions

Complex	Nucleophile	Wavelength (λ) (nm) Stopped-flow	UV-Visible
PtL2	**TU**	300	320
	DMTU	303	320
	TMTU	363	335
PtL3	**TU**	298	320
	DMTU	300	320
	TMTU	362	335
PtL4	**TU**	290	320
	DMTU	292	320
	TMTU	355	335
PtL5	**TU**	305	320
	DMTU	305	320
	TMTU	363	335
PtL6	**TU**	302	320
	DMTU	305	320
	TMTU	363	335

Table S2: Average observed rate constants, $k_{obs(1)}$, s^{-1}, for the displacement of the aqua ligands in PtL2 with the nucleophiles, at pH = 2.0, T = 298.15 K, I = 0.1 M $NaClO_4$.

TU		DMTU		TMTU	
Conc., M	$k_{obs(1)}$ (s^{-1})	Conc., M	$k_{obs(1)}$ (s^{-1})	Conc., M	$k_{obs(1)}$ (s^{-1})
0.06767	2.51096	0.06767	2.22029	0.06767	0.91433
0.05414	2.00193	0.05414	1.76683	0.05414	0.73637
0.04060	1.49424	0.04060	1.34718	0.04060	0.54065
0.02707	0.97325	0.02707	0.88399	0.02707	0.37482
0.01353	0.47818	0.01353	0.43177	0.01353	0.18377

Table S3: Average observed rate constants, $k_{obs(1)}$, s^{-1}, for the displacement of the aqua ligands in PtL3 with the nucleophiles, at pH = 2.0, T = 298.15 K, I = 0.1 M $NaClO_4$.

TU		DMTU		TMTU	
Conc., M	$k_{obs(1)}$ (s^{-1})	Conc., M	$k_{obs(1)}$ (s^{-1})	Conc., M	$k_{obs(1)}$ (s^{-1})
0.06767	1.47659	0.06767	1.19614	0.06767	0.64526
0.05414	1.16443	0.05414	0.94017	0.05414	0.53802
0.04060	0.90321	0.04060	0.70801	0.04060	0.40478
0.02707	0.57557	0.02707	0.44803	0.02707	0.26212
0.01353	0.26107	0.01353	0.21551	0.01353	0.10746

Table S4: Average observed rate constants, $k_{obs(1)}$, s^{-1}, for the displacement of the aqua ligands in PtL4 with the nucleophiles, at pH = 2.0, T = 298.15 K, I = 0.1 M $NaClO_4$.

TU		DMTU		TMTU	
Conc., M	$k_{obs(1)}$ (s^{-1})	Conc., M	$k_{obs(1)}$ (s^{-1})	Conc., M	$k_{obs(1)}$ (s^{-1})
0.06767	1.10612	0.06767	0.91759	0.06767	0.42164
0.05414	0.87857	0.05414	0.73711	0.05414	0.32454
0.04060	0.64594	0.04060	0.55036	0.04060	0.22417
0.02707	0.43478	0.02707	0.36521	0.02707	0.13206
0.01353	0.20861	0.01353	0.18141	0.01353	0.04116

Table S5: Average observed rate constants, $k_{obs(1)}$, s^{-1}, for the displacement of the aqua ligands in PtL5 with the nucleophiles, at pH = 2.0, T = 298.15 K, I = 0.1 M $NaClO_4$.

TU		DMTU		TMTU	
Conc., M	$k_{obs(1)}$ (s^{-1})	Conc., M	$k_{obs(1)}$ (s^{-1})	Conc., M	$k_{obs(1)}$ (s^{-1})
0.06767	0.94658	0.06767	1.03145	0.06767	0.42850
0.05414	0.78492	0.05414	0.84216	0.05414	0.33427
0.04060	0.64649	0.04060	0.64524	0.04060	0.25431
0.02707	0.49981	0.02707	0.47911	0.02707	0.17346
0.01353	0.34995	0.01353	0.30294	0.01353	0.08759

Table S6: Average observed rate constants, $k_{obs(1)}$, s^{-1}, for the displacement of the aqua ligands in PtL6 with the nucleophiles, at pH = 2.0, T = 298.15 K, I = 0.1 M $NaClO_4$.

TU		DMTU		TMTU	
Conc., M	$k_{obs(1)}$ (s^{-1})	Conc., M	$k_{obs(1)}$ (s^{-1})	Conc., M	$k_{obs(1)}$ (s^{-1})
0.06767	0.86819	0.06767	0.83580	0.06767	0.34655
0.05414	0.73014	0.05414	0.67843	0.05414	0.27283
0.04060	0.59426	0.04060	0.51663	0.04060	0.21317
0.02707	0.45489	0.02707	0.36303	0.02707	0.13459
0.01353	0.31510	0.01353	0.20789	0.01353	0.06650

Table S7: Average observed rate constants, $k_{obs(2)}$, s^{-1}, for the dechelation of the linker in PtL2 with the nucleophiles, at pH = 2.0, T = 298.15 K, I = 0.1 M $NaClO_4$.

TU		DMTU		TMTU	
Conc., M	$k_{obs(2)}$ (s^{-1})	Conc., M	$k_{obs(2)}$ (s^{-1})	Conc., M	$k_{obs(2)}$ (s^{-1})
0.06767	0.00224	0.06767	0.00404	0.06767	0.00070
0.05414	0.00165	0.05414	0.00315	0.05414	0.00056
0.04060	0.0010	0.04060	0.00214	0.04060	0.00042
0.02707	0.00045	0.02707	0.00135	0.02707	0.00029
0.01353	0.00011	0.01353	0.00038	0.01353	0.00014

Table S8: **Average observed rate constants, $k_{obs(2)}$, s^{-1}, for the dechelation of the linker in PtL3 with the nucleophiles, at pH = 2.0, T = 298.15 K, I = 0.1 M $NaClO_4$.**

TU		DMTU		TMTU	
Conc., M	$k_{obs(2)}$ (s^{-1})	Conc., M	$k_{obs(2)}$ (s^{-1})	Conc., M	$k_{obs(2)}$ (s^{-1})
0.06767	0.00413	0.06767	0.00156	0.06767	0.00150
0.05414	0.00310	0.05414	0.00122	0.05414	0.00115
0.04060	0.00221	0.04060	0.00083	0.04060	0.00080
0.02707	0.00110	0.02707	0.00046	0.02707	0.00044
0.01353	0.00019	0.01353	0.00011	0.01353	0.00010

Table S9: **Average observed rate constants, $k_{obs(2)}$, s^{-1}, for the substitution of the aqua ligands in PtL4 with the nucleophiles, at pH = 2.0, T = 298.15 K, I = 0.1 M $NaClO_4$.**

TU		DMTU		TMTU	
Conc., M	$k_{obs(2)}$ (s^{-1})	Conc., M	$k_{obs(2)}$ (s^{-1})	Conc., M	$k_{obs(2)}$ (s^{-1})
0.06767	0.00654	0.06767	0.00446	0.06767	0.00250
0.05414	0.00498	0.05414	0.00348	0.05414	0.00201
0.04060	0.00410	0.04060	0.00252	0.04060	0.00147
0.02707	0.00217	0.02707	0.00155	0.02707	0.00091
0.01353	0.00070	0.01353	0.00092	0.01353	0.00042

Table S10: **Average observed rate constants, $k_{obs(2)}$, s^{-1}, for the dechelation of the linker in PtL5 with the nucleophiles, at pH = 2.0, T = 298.15 K, I = 0.1 M $NaClO_4$.**

TU		DMTU		TMTU	
Conc., M	$k_{obs(2)}$ (s^{-1})	Conc., M	$k_{obs(2)}$ (s^{-1})	Conc., M	$k_{obs(2)}$ (s^{-1})
0.06767	0.00309	0.06767	0.00184	0.06767	0.00060
0.05414	0.00241	0.05414	0.00145	0.05414	0.00049
0.04060	0.00172	0.04060	0.00103	0.04060	0.00038
0.02707	0.00103	0.02707	0.00058	0.02707	0.00027
0.01353	0.00036	0.01353	0.00021	0.01353	0.00016

Table S11: Average observed rate constants, $k_{obs(2)}$, s^{-1}, for the substitution of the aqua ligands in PtL6 with the nucleophiles, at pH = 2.0, T = 298.15 K, I = 0.1 M $NaClO_4$.

TU		DMTU		TMTU	
Conc., M	$k_{obs(2)}$ (s^{-1})	Conc., M	$k_{obs(2)}$ (s^{-1})	Conc., M	$k_{obs(2)}$ (s^{-1})
0.06767	0.00469	0.06767	0.00194	0.06767	0.00185
0.05414	0.00359	0.05414	0.00150	0.05414	0.00163
0.04060	0.00251	0.04060	0.00111	0.04060	0.00143
0.02707	0.00143	0.02707	0.00067	0.02707	0.00118
0.01353	0.00044	0.01353	0.00028	0.01353	0.00095

Table S12: Average observed rate constants, $k_{obs(3)}$, s^{-1}, for the substitution of the aqua ligands in PtL4 with the nucleophiles, at pH = 2.0, T = 298.15 K, I = 0.1 M $NaClO_4$.

TU		DMTU	
Conc., M	$k_{obs(2)}$ (s^{-1})	Conc., M	$k_{obs(2)}$ (s^{-1})
0.06767	0.00043892	0.06767	0.00022370
0.05414	0.00036983	0.05414	0.00018269
0.04060	0.00030034	0.04060	0.00014294
0.02707	0.00023688	0.02707	0.00010620
0.01353	0.00015745	0.01353	0.00006588

Table S13: Average observed rate constants, $k_{obs(2)}$, s^{-1}, for the substitution of the aqua ligands in PtL6 with the nucleophiles, at pH = 2.0, T = 298.15 K, I = 0.1 M $NaClO_4$.

TU		DMTU	
Conc., M	$k_{obs(2)}$ (s^{-1})	Conc., M	$k_{obs(2)}$ (s^{-1})
0.06767	0.000044457	0.06767	0.000055227
0.05414	0.000036853	0.05414	0.000046590
0.04060	0.000030241	0.04060	0.000036916
0.02707	0.000022912	0.02707	0.000027835
0.01353	0.000015720	0.01353	0.000020254

Table S14: Temperature dependence of k_2/$M^{-1}s^{-1}$, for the displacement of the aqua ligands in PtL2 by the nucleophiles at 120-fold at pH = 2.0, I = 0.1 M $NaClO_4$

TU		DMTU		TMTU	
1/T (K^{-1})	ln(k_2/T)	1/T (K^{-1})	ln(k_2/T)	1/T (K^{-1})	ln(k_2/T)
0.00325	-4.64485	0.00325	-4.81834	0.00325	-5.80987
0.00330	-4.96562	0.00330	-5.10753	0.00330	-6.03467
0.00336	-5.29547	0.00336	-5.39908	0.00336	-6.31208
0.00341	-5.63597	0.00341	-5.70705	0.00341	-6.59488
0.00347	-5.98855	0.00347	-6.04632	0.00347	-6.87473

Table S15: Temperature dependence of k_2/$M^{-1}s^{-1}$, for the displacement of the aqua ligands in PtL3 by the nucleophiles at 120-fold at pH = 2.0, I = 0.1 M $NaClO_4$

TU		DMTU		TMTU	
1/T (K^{-1})	ln(k_2/T)	1/T (K^{-1})	ln(k_2/T)	1/T (K^{-1})	ln(k_2/T)
0.00325	-5.35899	0.00325	-5.76252	0.00325	-6.01404
0.00330	-5.59484	0.00330	-5.88652	0.00330	-6.29297
0.00336	-5.79889	0.00336	-6.04239	0.00336	-6.60151
0.00341	-6.06392	0.00341	-6.19096	0.00341	-6.94986
0.00347	-6.36160	0.00347	-6.32252	0.00347	-7.29111

Table S16: Temperature dependence of k_2/$M^{-1}s^{-1}$, for the displacement of the aqua ligands in PtL4 by the nucleophiles at 120-fold at pH = 2.0, I = 0.1 M $NaClO_4$

TU		DMTU		TMTU	
1/T (K^{-1})	ln(k_2/T)	1/T (K^{-1})	ln(k_2/T)	1/T (K^{-1})	ln(k_2/T)
0.00325	-5.64941	0.00325	-5.77924	0.00325	-6.66437
0.00330	-5.86293	0.00330	-6.02583	0.00330	-6.90796
0.00336	-6.13415	0.00336	-6.29428	0.00336	-7.19244
0.00341	-6.38471	0.00341	-6.55584	0.00341	-7.46058
0.00347	-6.65256	0.00347	-6.85609	0.00347	-7.72969

Table S17: Temperature dependence of k_2/$M^{-1}s^{-1}$, for the displacement of the aqua ligands in PtL5 by the nucleophiles at 120-fold at pH = 2.0, I = 0.1 M $NaClO_4$

TU		DMTU		TMTU	
1/T (K^{-1})	ln(k_2/T)	1/T (K^{-1})	ln(k_2/T)	1/T (K^{-1})	ln(k_2/T)
0.00325	-5.52510	0.00325	-5.48022	0.00325	-6.43019
0.00330	-5.73966	0.00330	-5.75781	0.00330	-6.73446
0.00336	-5.93927	0.00336	-6.13522	0.00336	-7.06629
0.00341	-6.16591	0.00341	-6.44271	0.00341	-7.41237
0.00347	-6.42657	0.00347	-6.81639	0.00347	-7.74960

Table S18: **Temperature dependence of $k_2/M^{-1}s^{-1}$, for the displacement of the aqua ligands in PtL6 by the nucleophiles at 120-fold at pH = 2.0, I = 0.1 M $NaClO_4$**

TU		DMTU		TMTU	
1/T (K^{-1})	ln(k_2/T)	1/T (K^{-1})	ln(k_2/T)	1/T (K^{-1})	ln(k_2/T)
0.00325	-5.89373	0.00325	-6.11154	0.00325	-6.35065
0.00330	-6.05289	0.00330	-6.23335	0.00330	-6.74529
0.00336	-6.21753	0.00336	-6.35752	0.00336	-7.24276
0.00341	-6.39268	0.00341	-6.47978	0.00341	-7.72905
0.00347	-6.56600	0.00347	-6.61352	0.00347	-8.26895

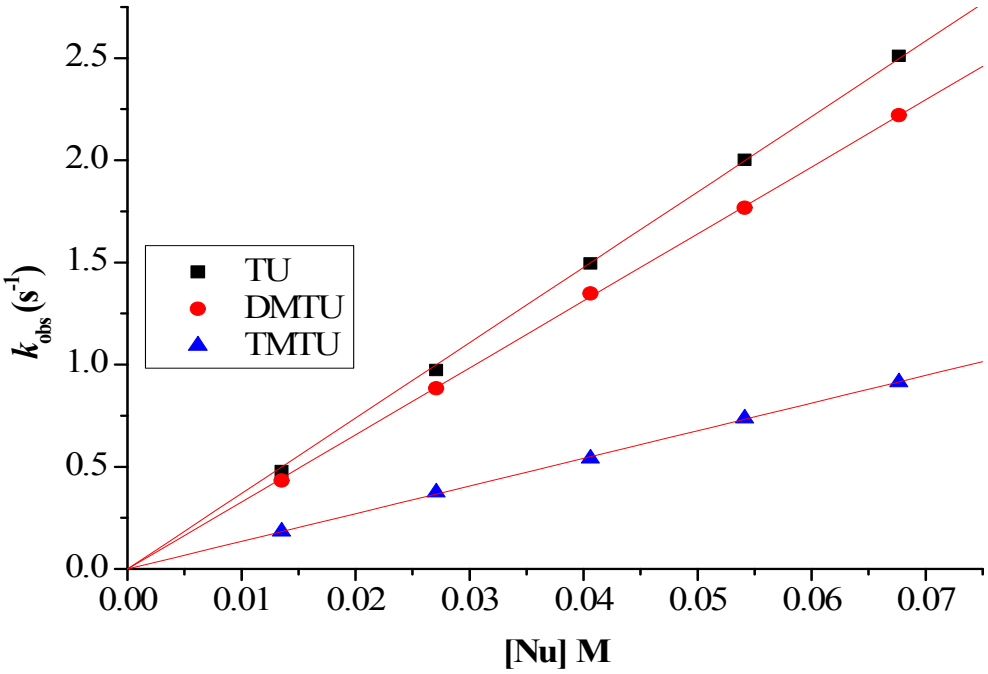

Figure S1: **Dependence of the *pseudo* first-order rate constants (k_{obs}) on the concentrations of the nucleophiles for the aqua substitution for PtL2 in $NaClO_4$ (I = 0.1 M) at 298.15 K.**

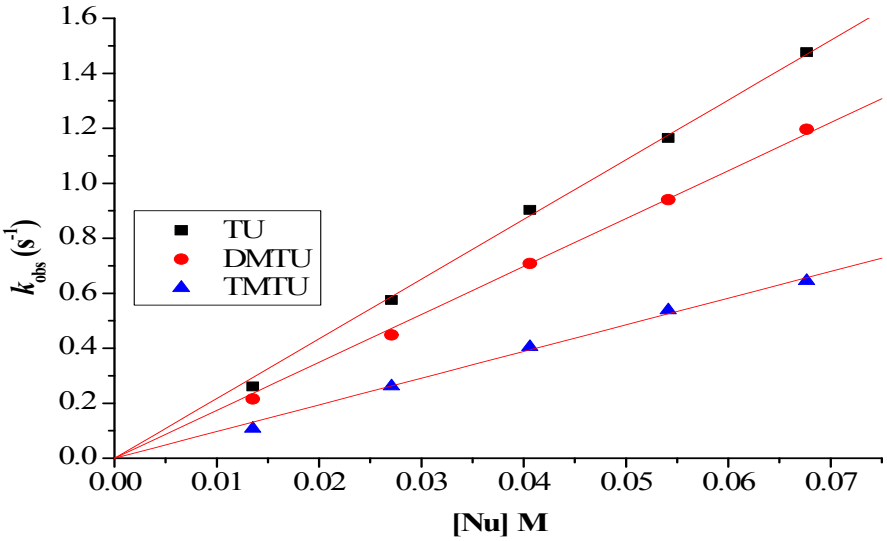

Figure S2: **Dependence of the *pseudo* first-order rate constants (k_{obs}) on the concentrations of the nucleophiles for the aqua substitution for PtL3 in $NaClO_4$ (I = 0.1 M) at 298.15 K.**

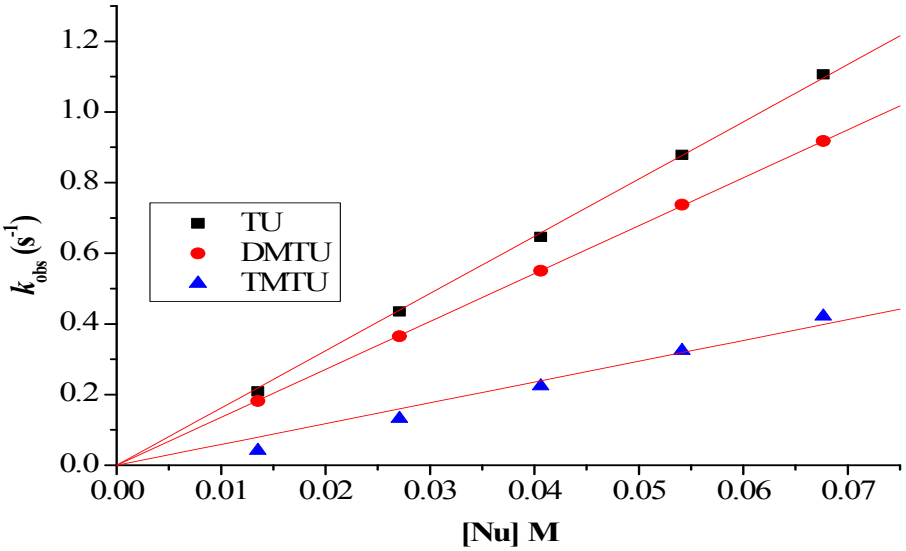

Figure S3: **Dependence of the *pseudo* first-order rate constants (k_{obs}) on the concentrations of the nucleophiles for the aqua substitution for PtL4 in $NaClO_4$ (I = 0.1 M) at 298.15 K.**

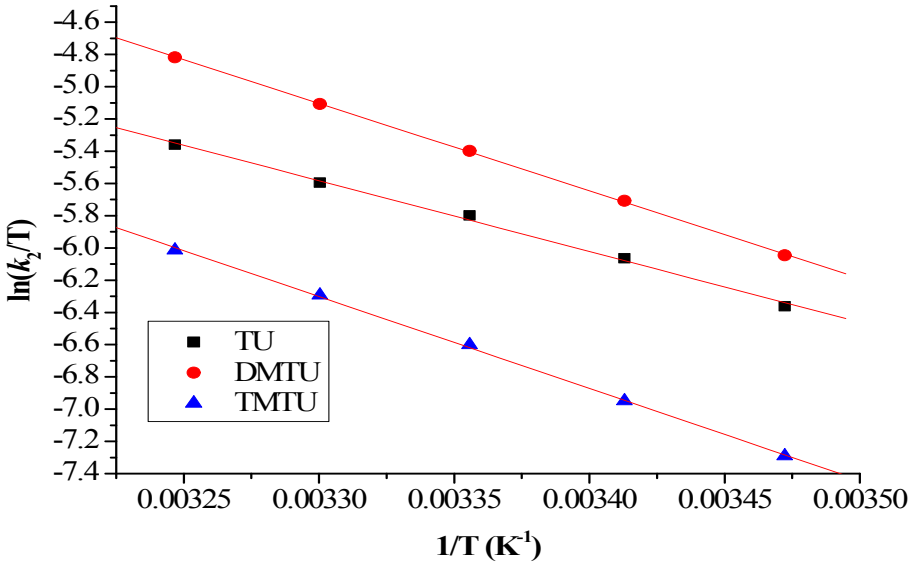

Figure S4: **Eyring plots obtained for PtL3 with the nucleophiles for the substitution reactions over the temperature range 288.15 – 308.15 K in $NaClO_4$ (*I* = 0.1 M).**

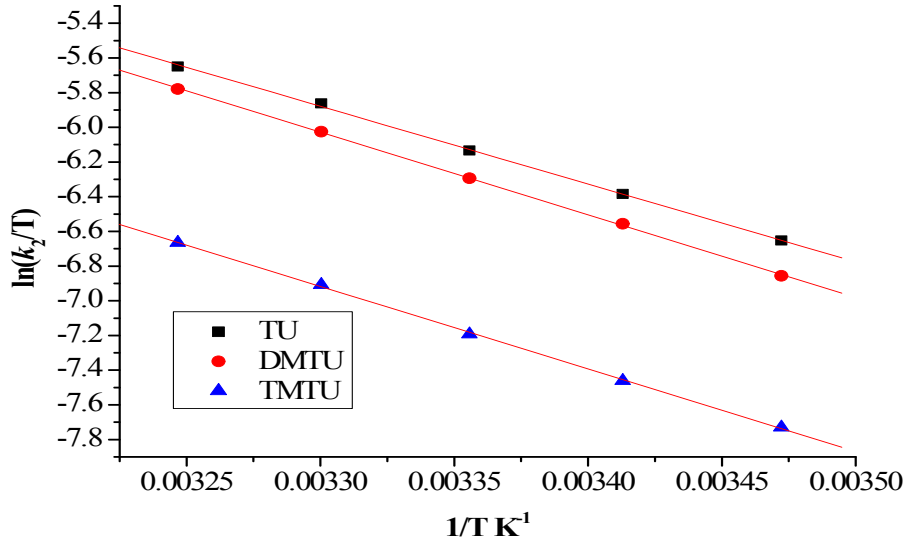

Figure S5: **Eyring plots obtained for PtL4 with the nucleophiles for the substitution reactions over the temperature range 288.15 – 308.15 K in $NaClO_4$ (*I* = 0.1 M).**

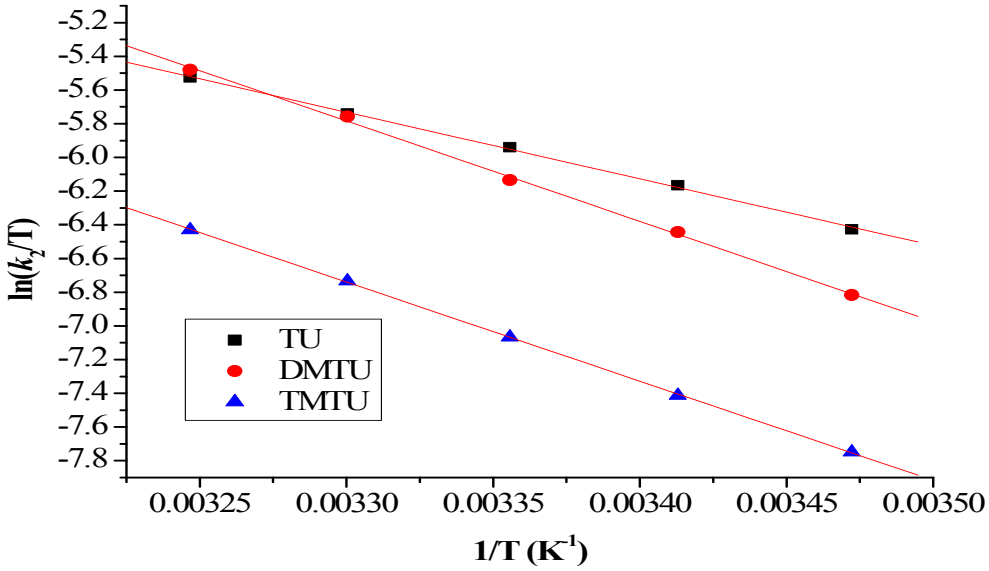

Figure S6: **Eyring plots obtained for PtL5 with the nucleophiles for the substitution reactions over the temperature range 288.15 – 308.15 K in $NaClO_4$ (I = 0.1 M).**

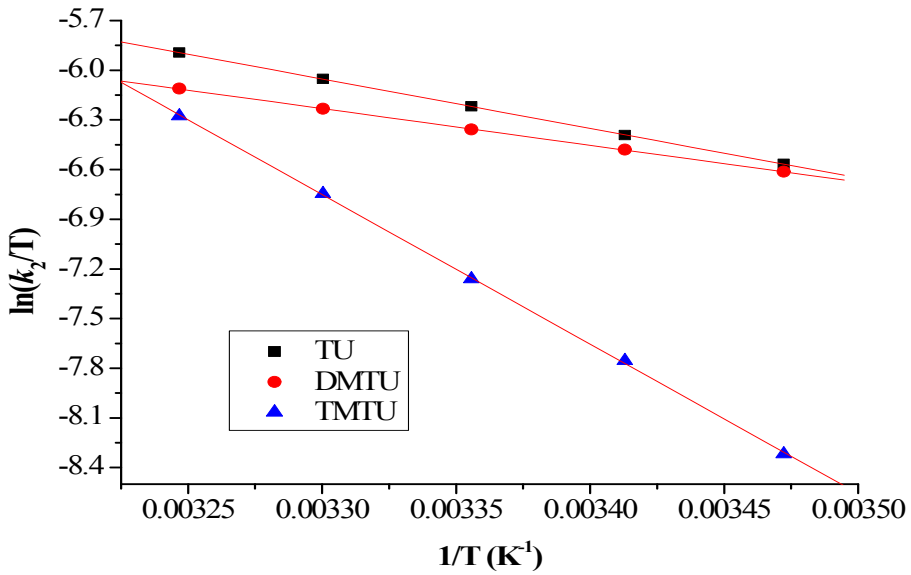

Figure S7: **Eyring plots obtained for PtL6 with the nucleophiles for the substitution reactions over the temperature range 288.15 – 308.15 K in $NaClO_4$ (I = 0.1 M).**

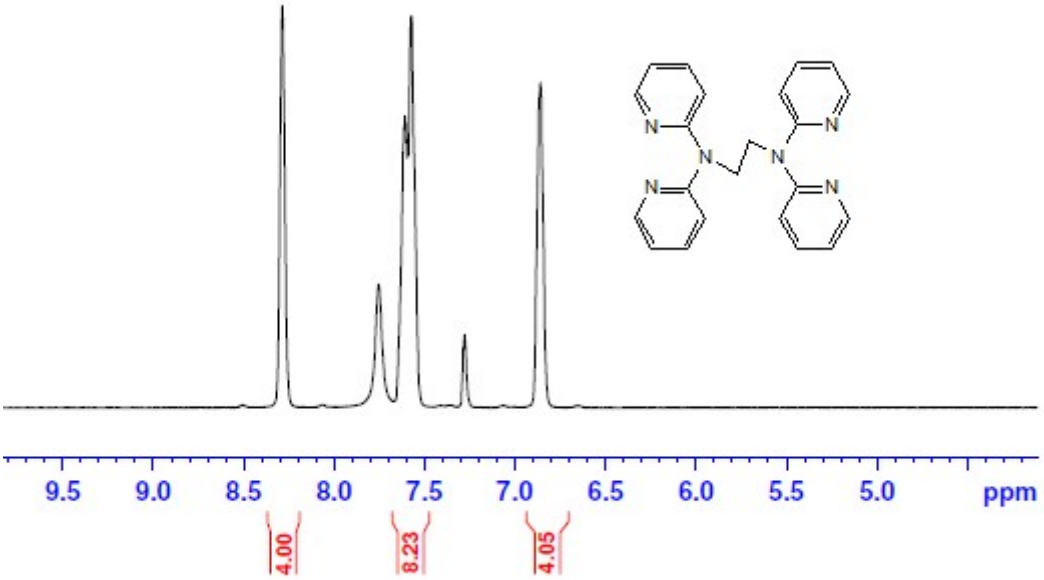

Figure S8: **^{1}H NMR spectrum of 1,2-*N,N'*-di-(2,2'-dipyridylamine)ethane (dpa_2En), in $CDCl_3$.**

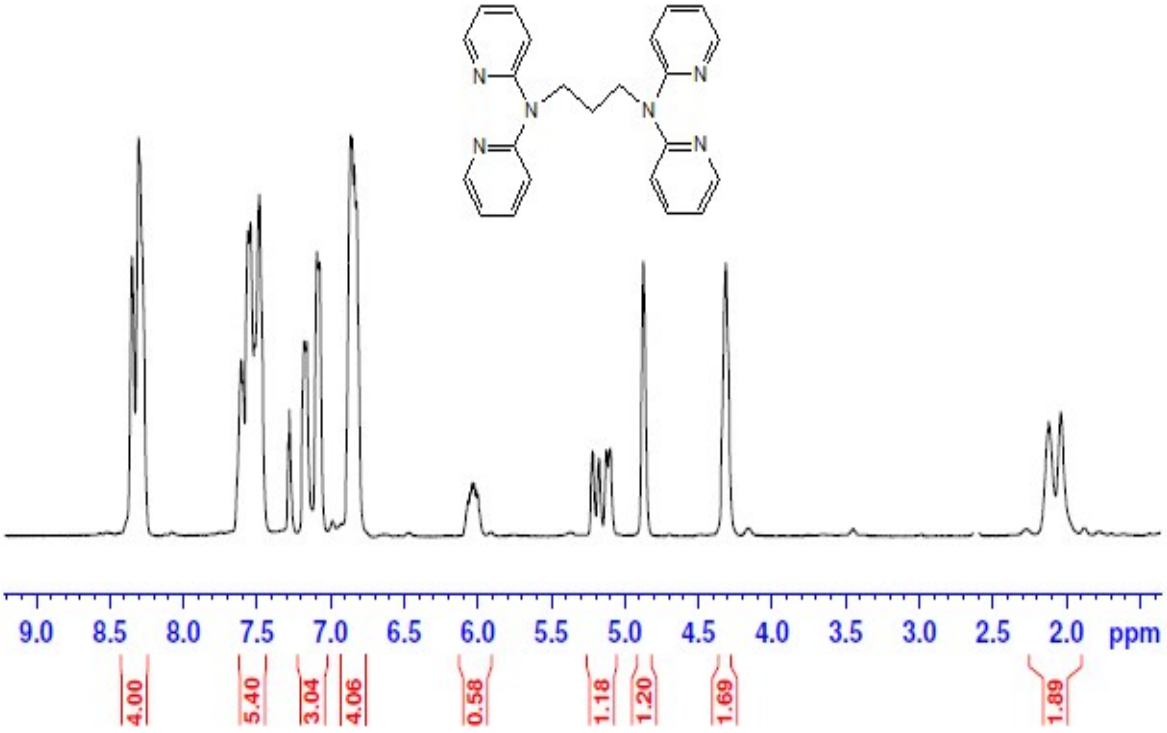

Figure S9: **^{1}H NMR spectrum of 1,3-*N,N'*-Di-(2,2'-dipyridylamine)propane (dpa_2Prop), in $CDCl_3$.**

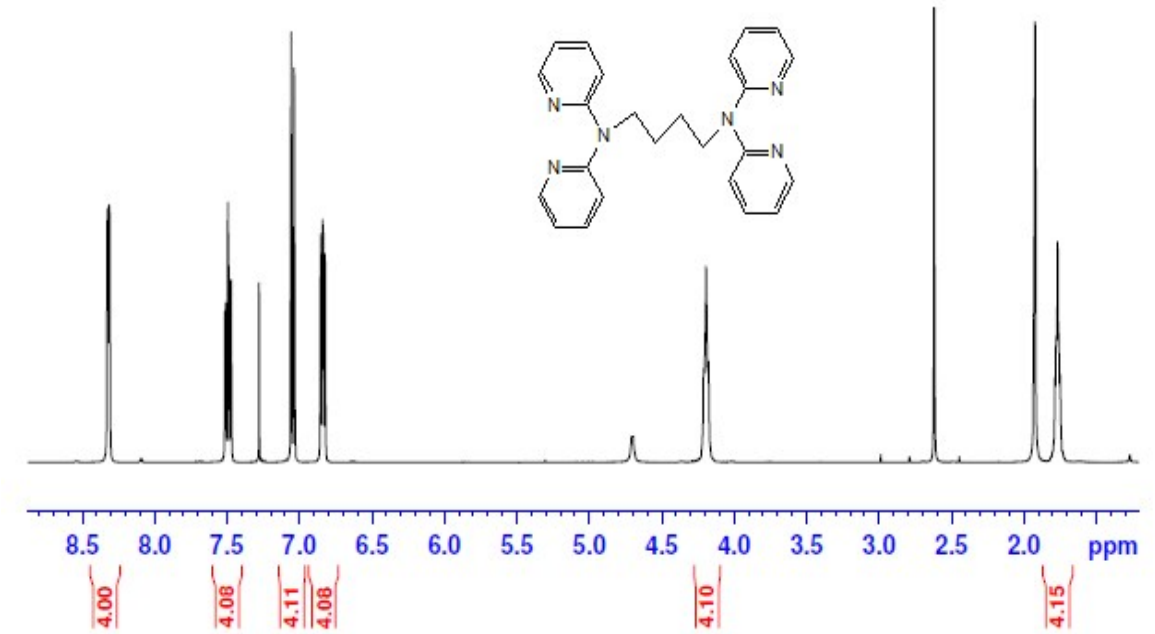

Figure S10: **^{1}H NMR spectrum of 1,4-*N,N'*-Di-(2,2'-dipyridylamine)butane (dpa_2But), in $CDCl_3$.**

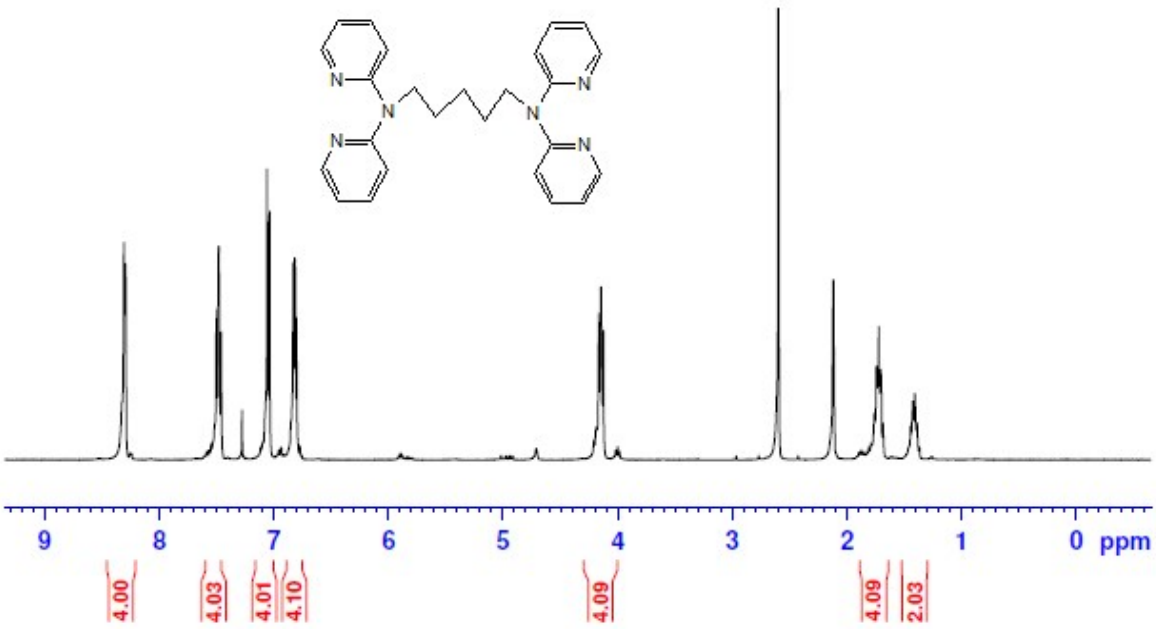

Figure S11: **^{1}H NMR spectrum of 1,5-*N,N'*-Di-(2,2'-dipyridylamine)pentane (dpa_2Pent), in $CDCl_3$.**

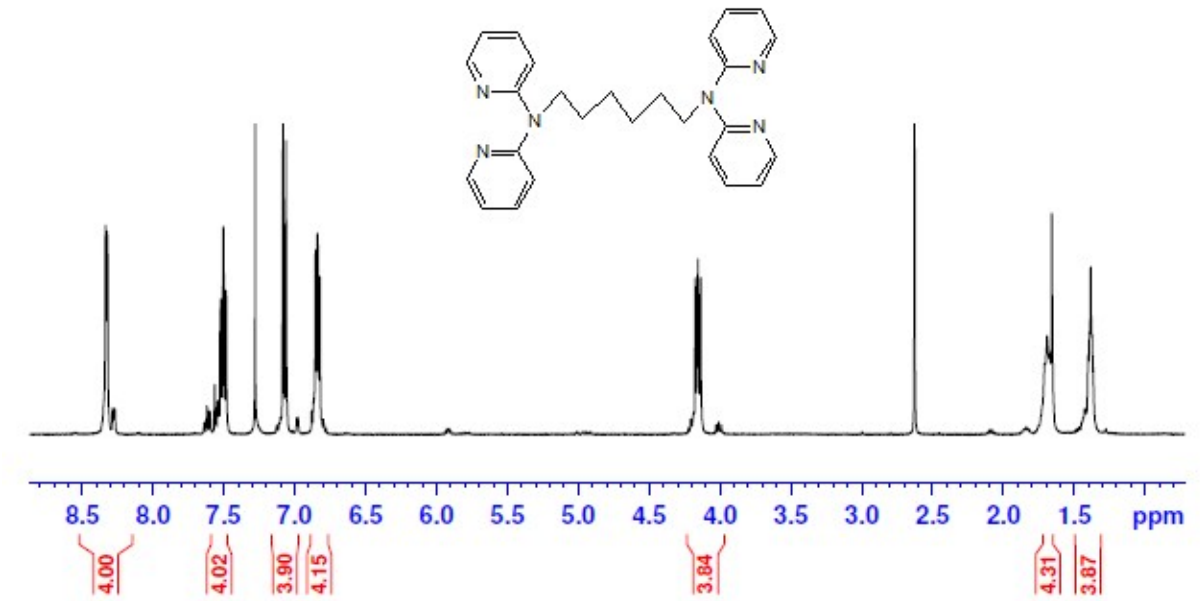

Figure S12: **^{1}H NMR spectrum of 1,6-*N,N'*-Di-(2,2'-dipyridylamine)hexane (dpa_2Hex), in $CDCl_3$.**

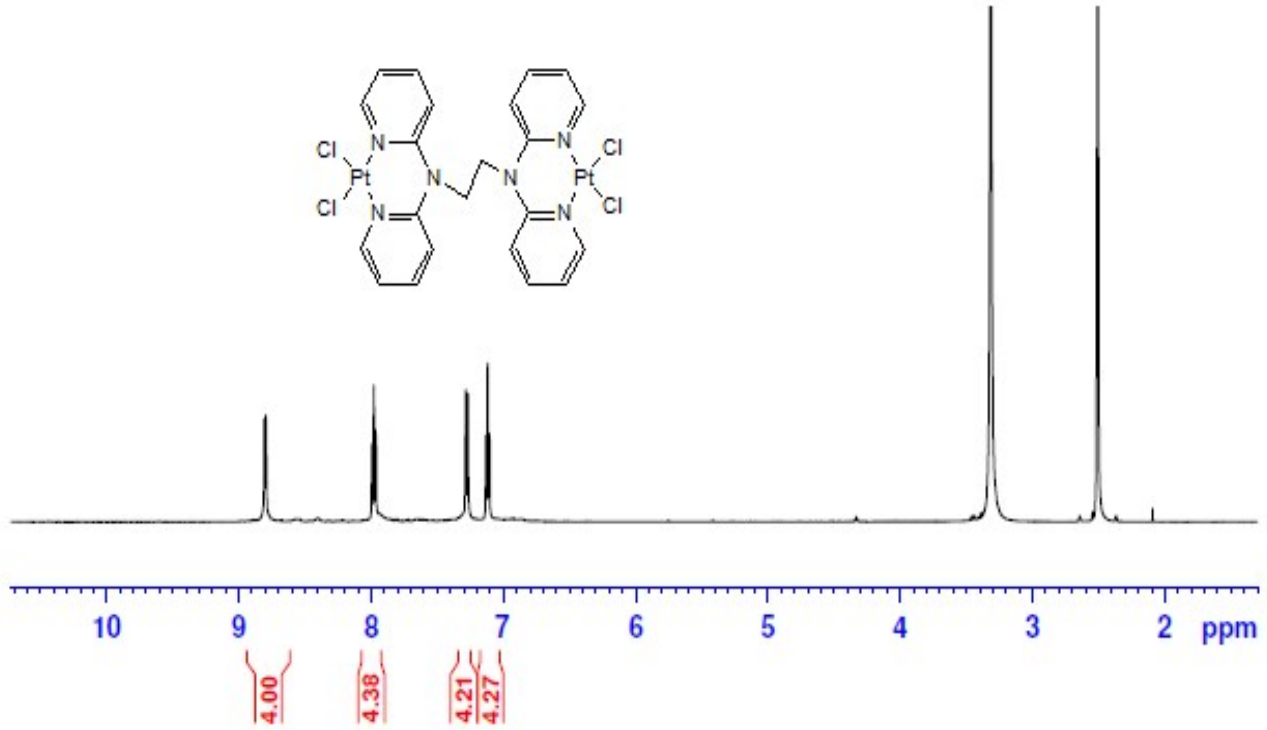

Figure S13: **^{1}H NMR spectrum of PtL2 in DMSO-d_6.**

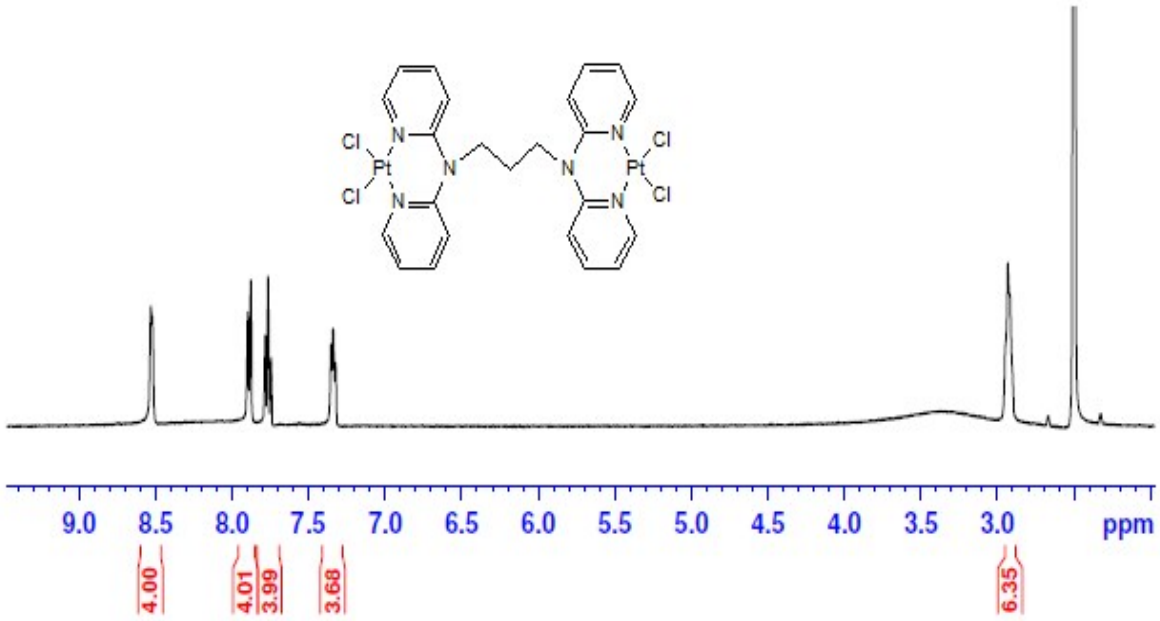

Figure S14: **^{1}H NMR spectrum of PtL3 in DMSO-d$_6$.**

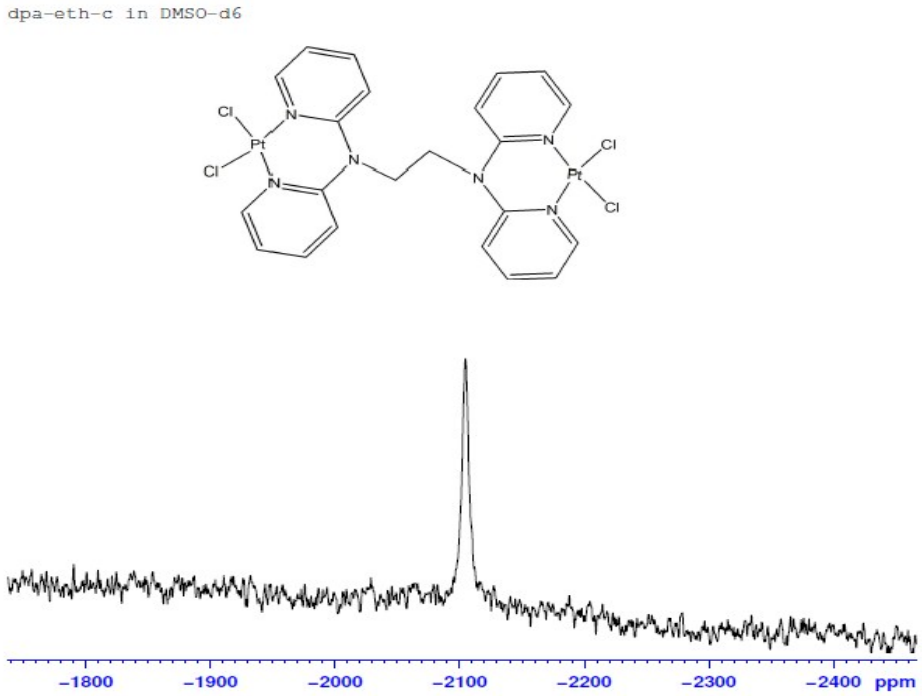

Figure S15: **^{195}Pt NMR spectrum of PtL2 in DMSO-*d*$_6$.**

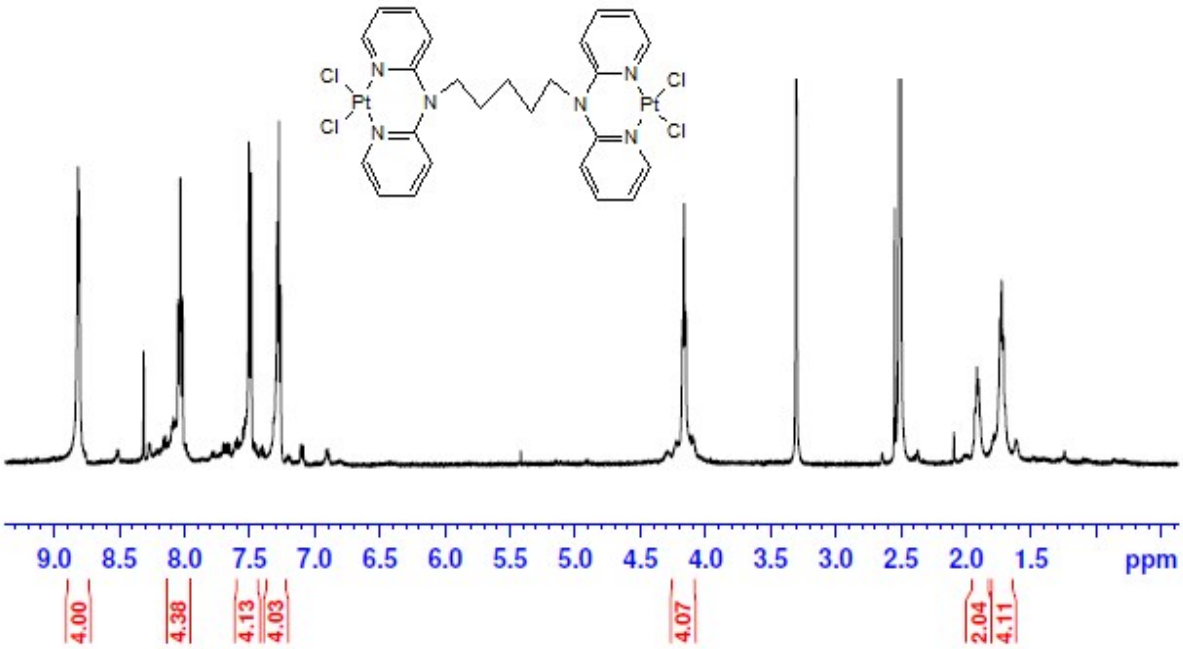

Figure S16: ^{1}H NMR spectrum of PtL5 in DMSO-d_6.

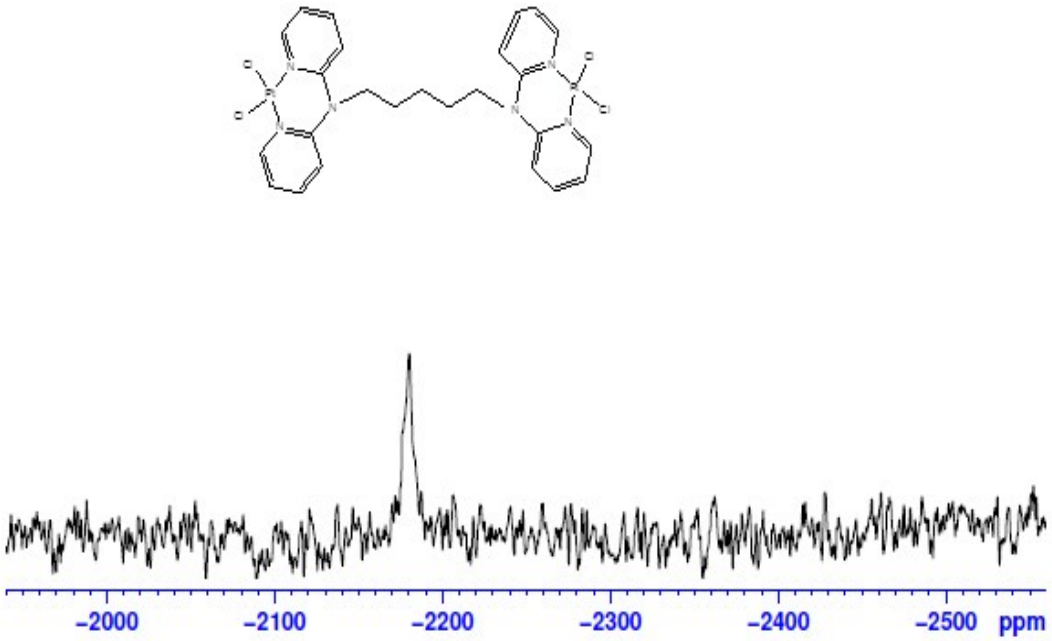

Figure S17: ^{195}Pt NMR spectrum of PtL5 in DMSO-d_6.

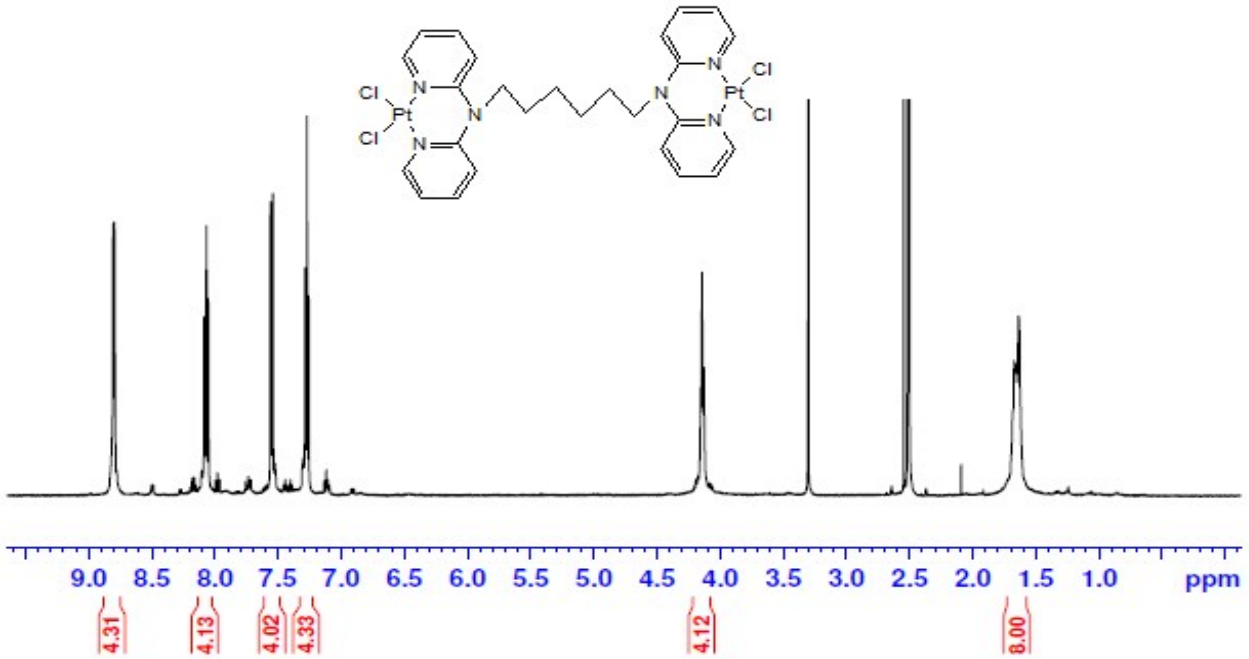

Figure S18: **^{1}H NMR spectrum of PtL6 in DMSO-d_6.**

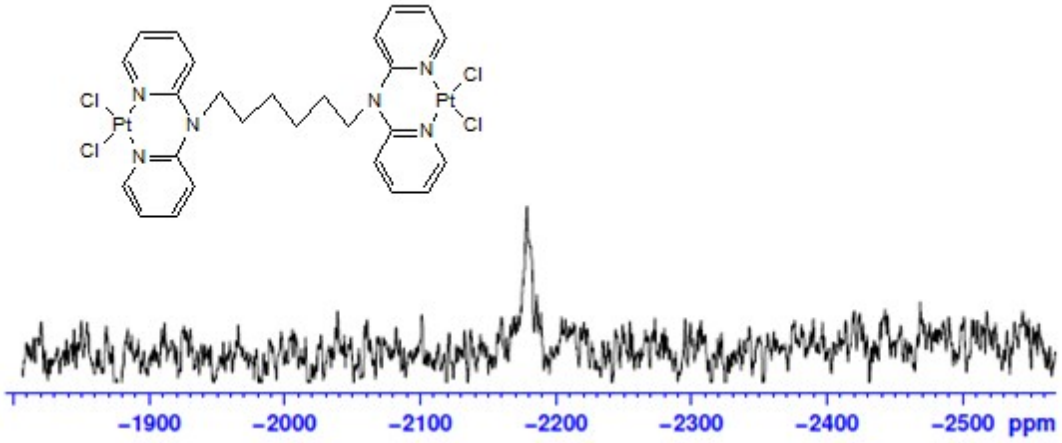

Figure S19: **^{195}Pt NMR spectrum of PtL6 in DMSO-d_6.**

Elemental Composition Report Page 1

Single Mass Analysis
Tolerance = 5.0 PPM / DBE: min = -1.5, max = 50.0
Element prediction: Off
Number of isotope peaks used for i-FIT = 3

Monoisotopic Mass, Even Electron Ions
3 formula(e) evaluated with 1 results within limits (all results (up to 1000) for each mass)
Elements Used:
C: 20-25 H: 20-25 N: 5-10
Grace Kinunda
dpa2 pnp 2 (0.017) Cm (1:31)

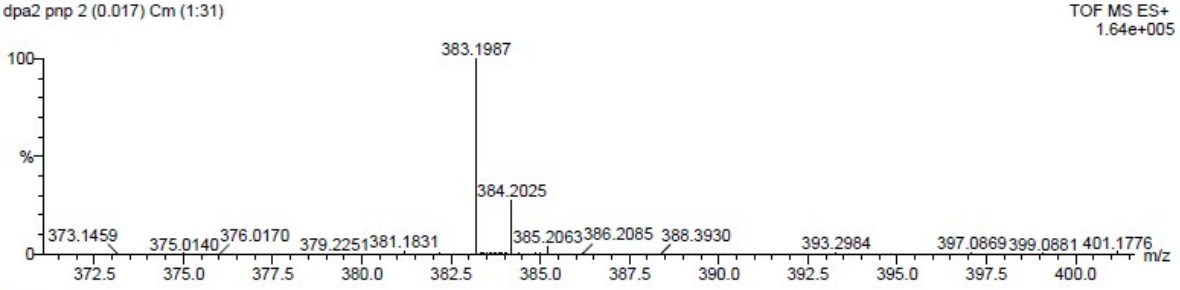

Minimum:				-1.5			
Maximum:		5.0	5.0	50.0			
Mass	Calc. Mass	mDa	PPM	DBE	i-FIT	i-FIT (Norm)	Formula
383.1987	383.1984	0.3	0.8	15.5	553.0	0.0	C23 H23 N6

Figure S20: TOF ESI mass spectrum of 1,3-*N,N'*-Di-(2,2'-dipyridylamine)propane (dpa_2Prop)

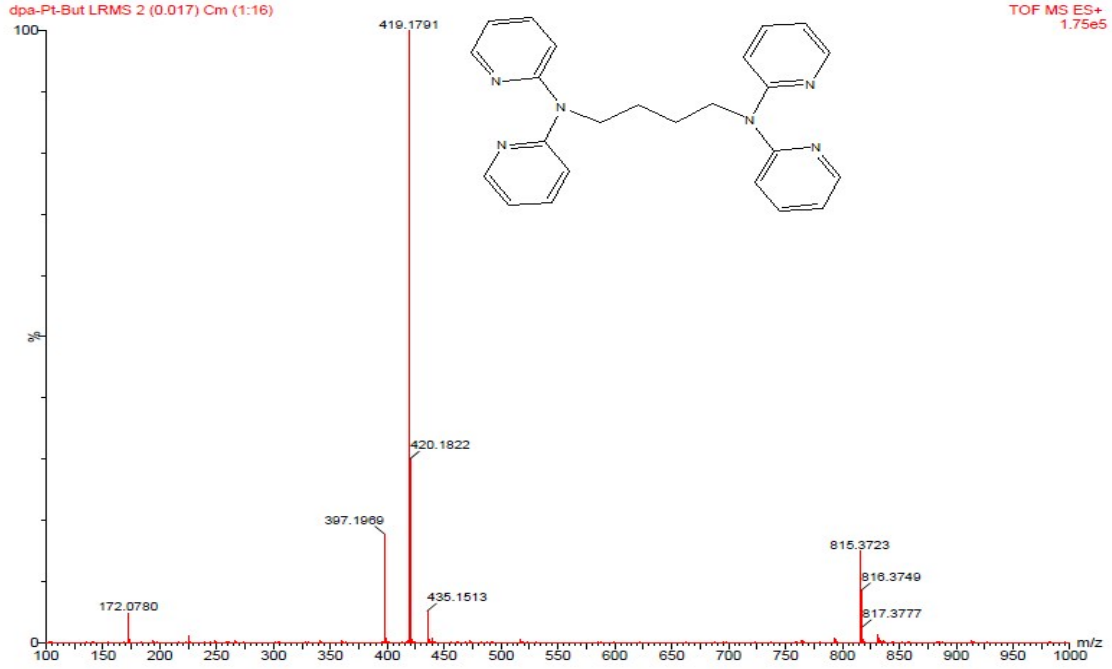

Figure S21: TOF ESI mass spectrum of 1,4-*N,N'*-Di-(2,2'-dipyridylamine)butane (dpa_2But)

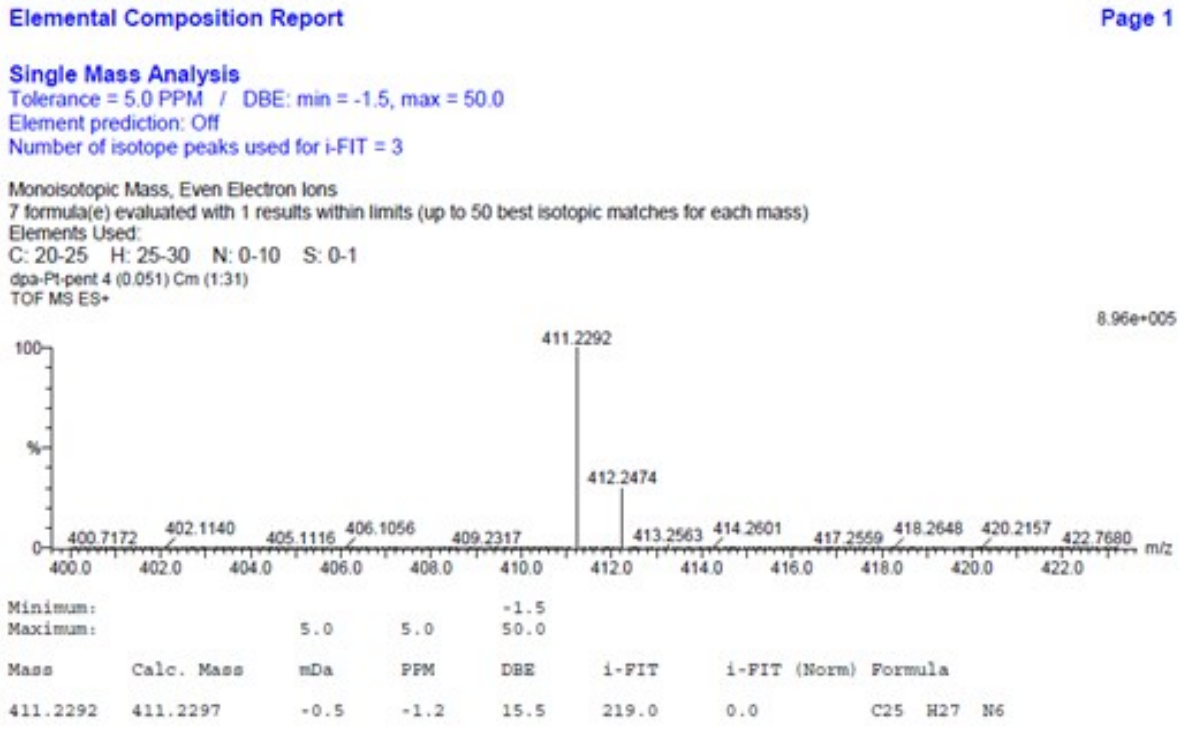

Figure S22: **TOF ESI mass spectrum of 1,5-*N,N'*-Di-(2,2'-dipyridylamine)pentane (dpa_2Pent)**

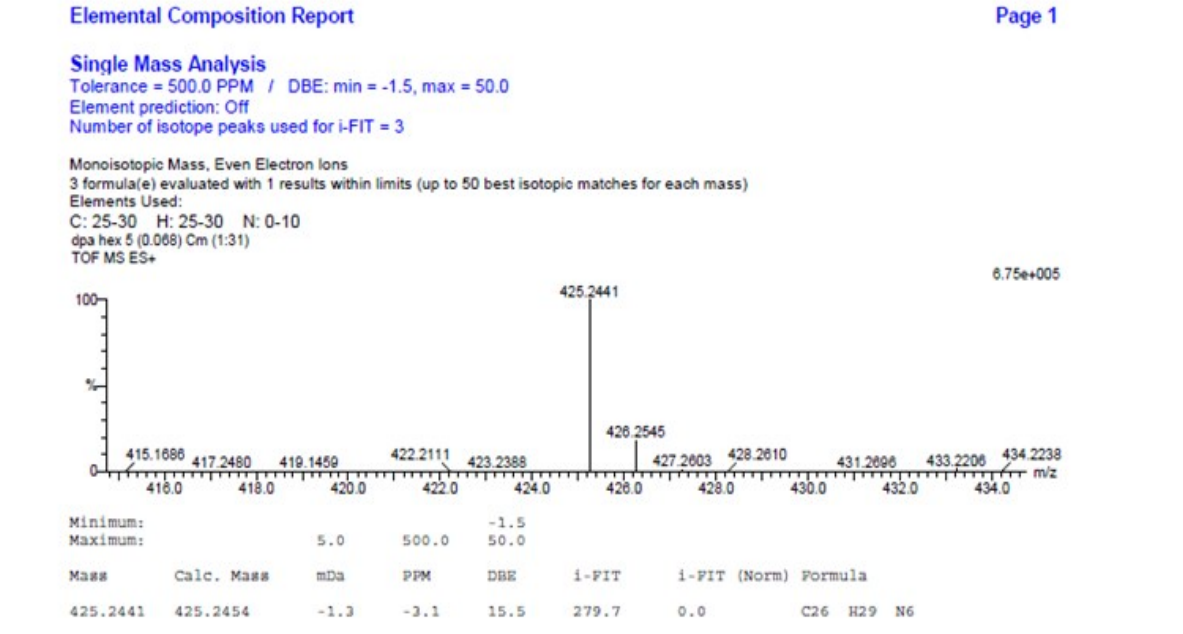

Figure S23: **TOF ESI mass spectrum of 1,6-*N,N'*-Di-(2,2'-dipyridylamine)hexane (dpa_2Hex)**

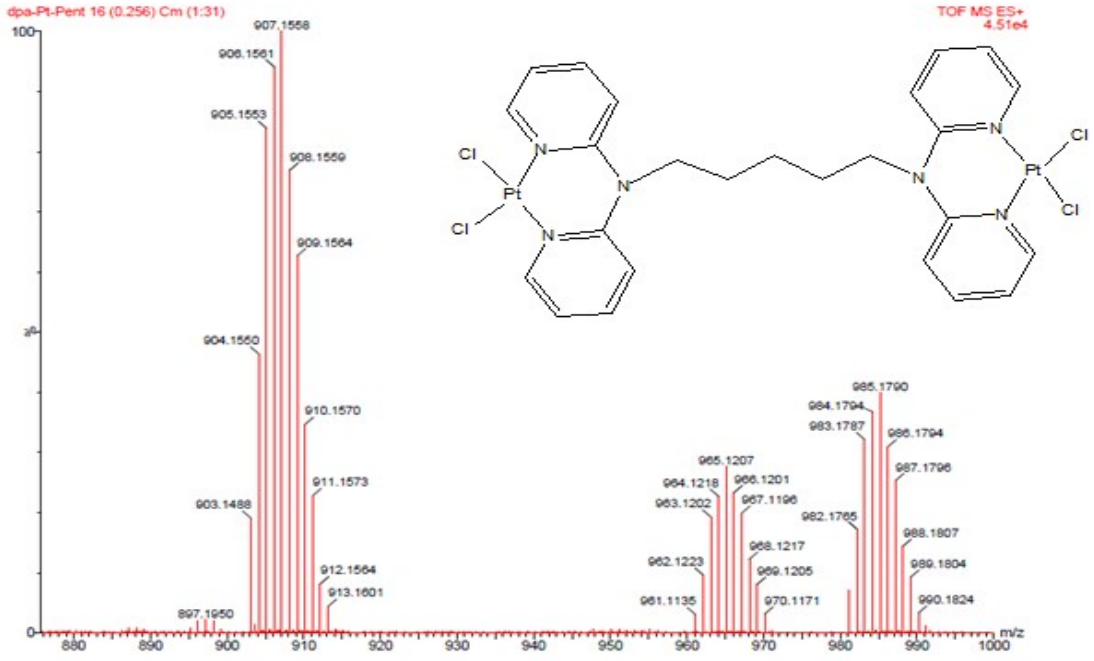

Figure S24: TOF ESI mass spectrum of PtL5

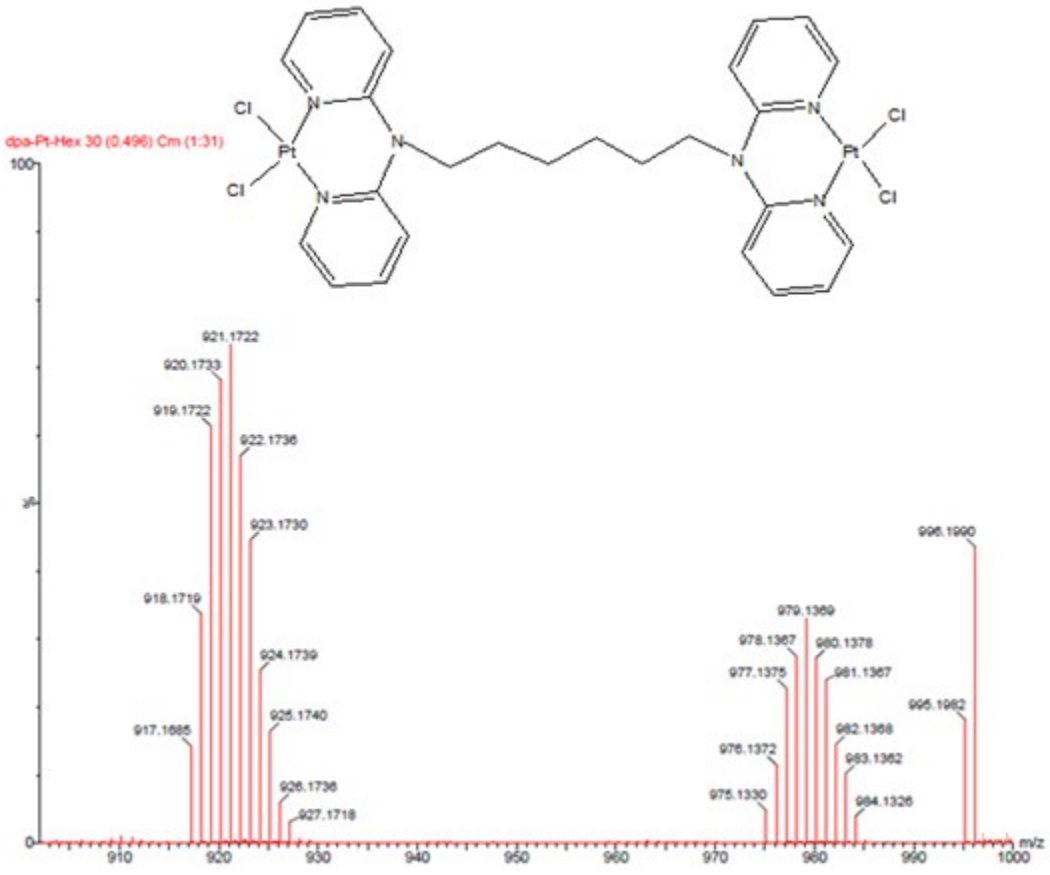

Figure S25: TOF ESI mass spectrum of PtL6

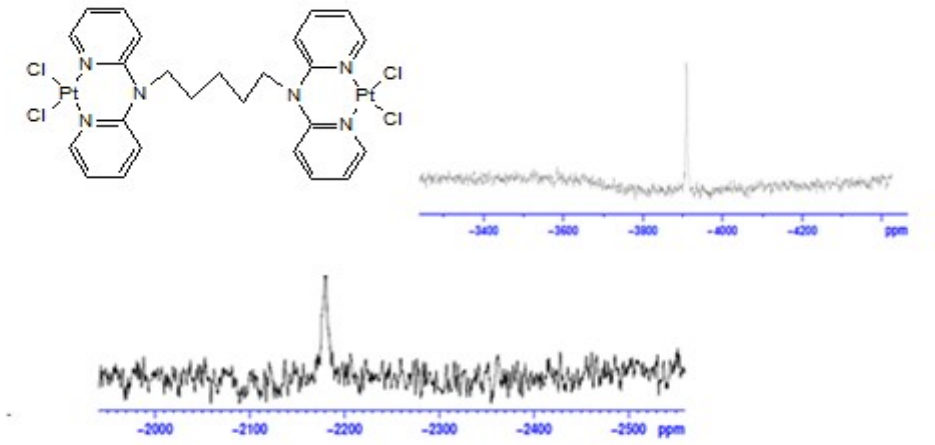

Figure S26: **^{195}Pt NMR spectrum of PtL5 in DMSO-d_6.**

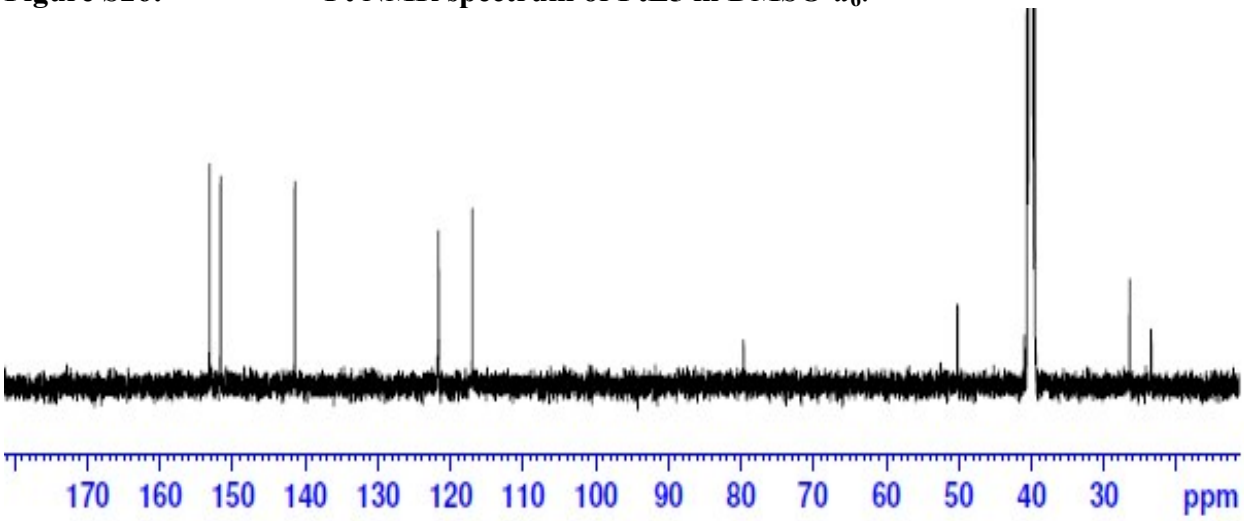

Figure S27: **^{13}C NMR spectrum for the complex PtL5 in DMSO-d_6.**

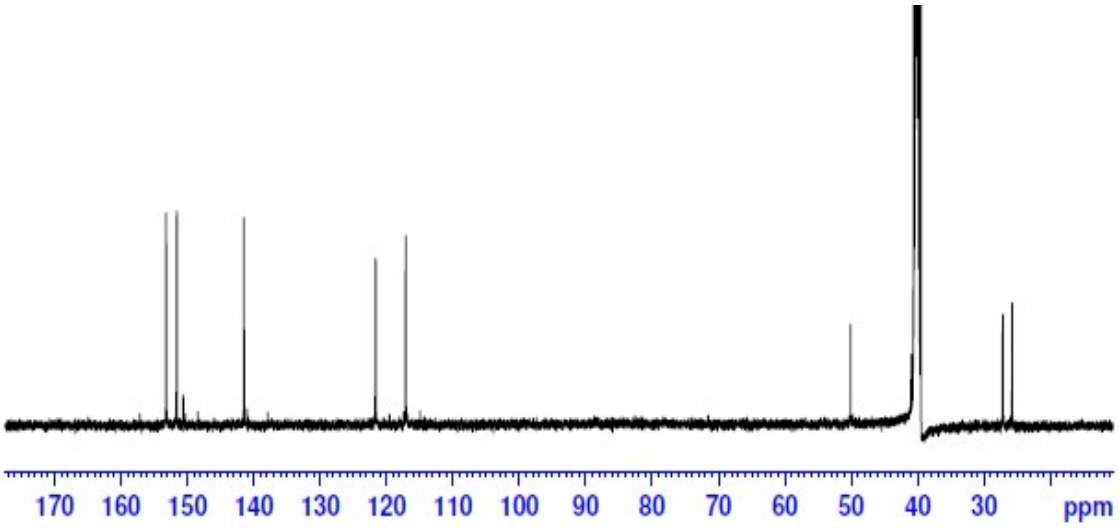

Figure S28: **^{13}C NMR spectrum for the complex PtL6 in DMSO-d_6.**

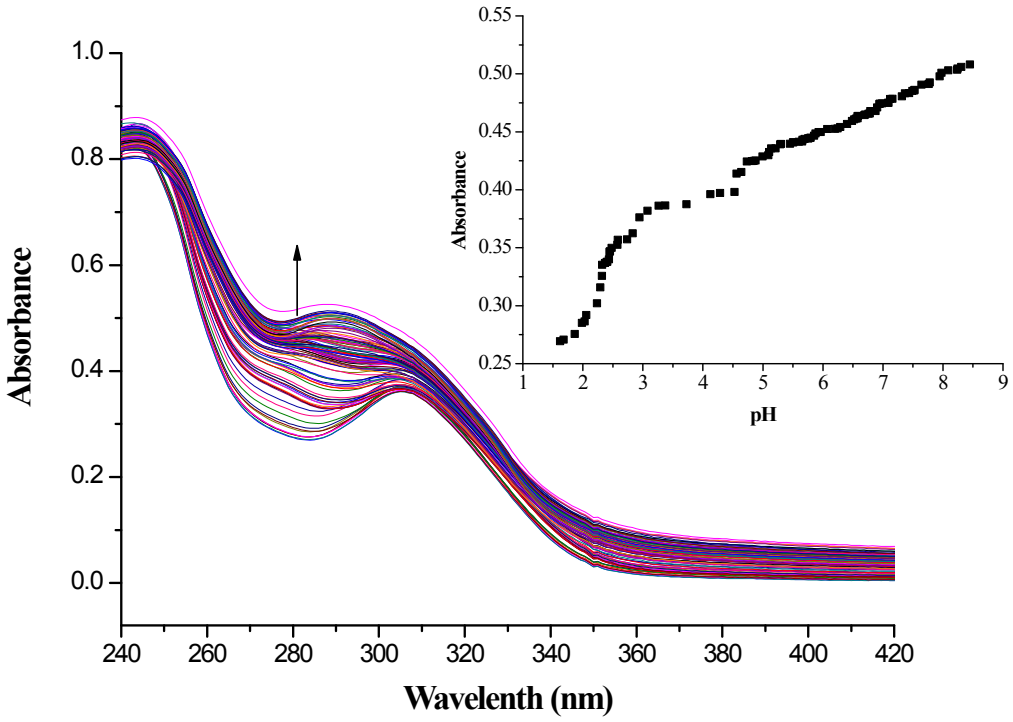

Figure S29: **UV/Vis spectral changes for the titration of PtL4 within the pH range of 1 to 9*; Inset* shows the titration curve at λ = 290 nm**

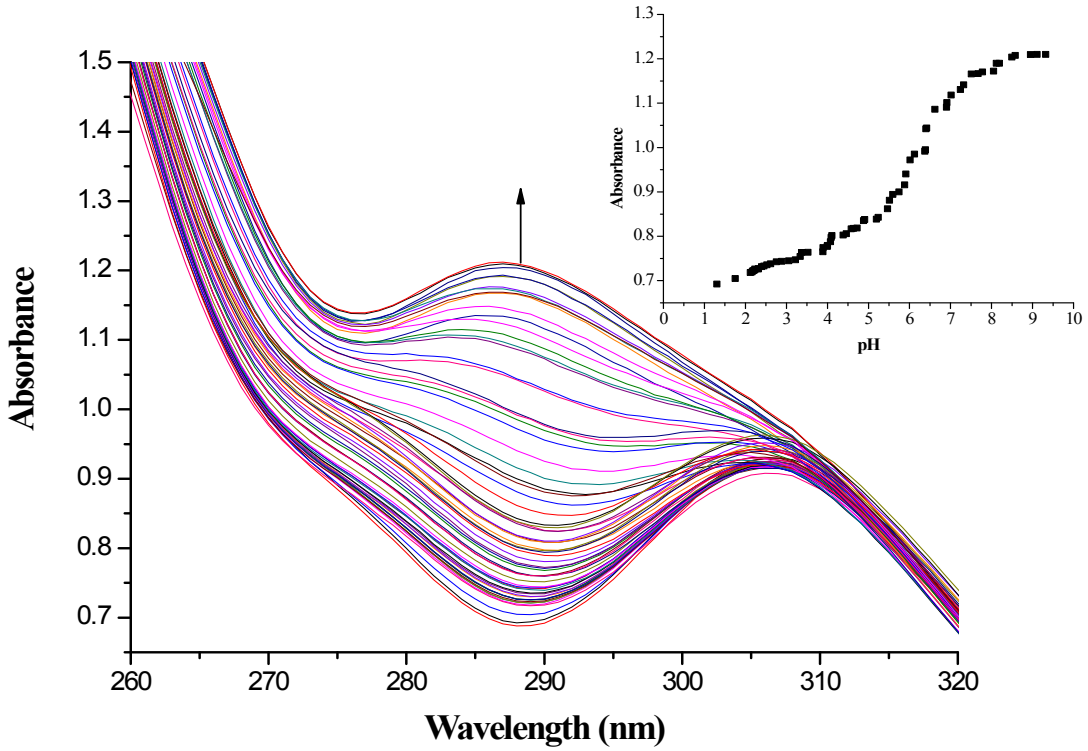

Figure S30: **UV/Vis spectral changes for the titration of PtL5 within the pH range of 1 to 10*; Inset* shows the titration curve at λ = 288 nm.**

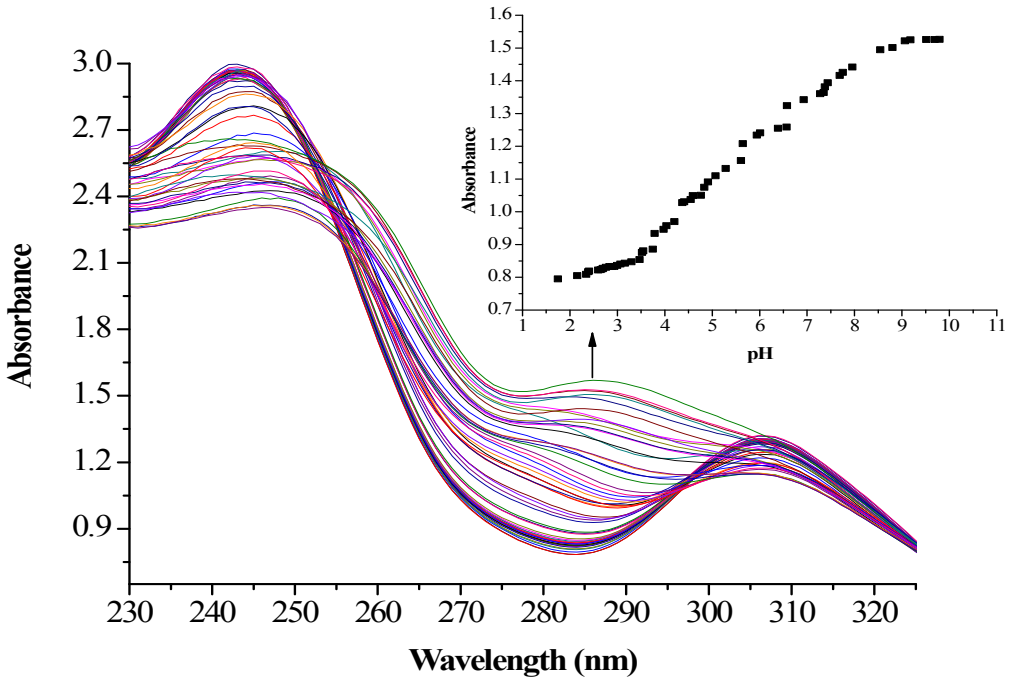

Figure S31: **UV/Vis spectral changes for the titration of PtL6 within the pH range of 1 to 10*; Inset* shows the titration curve at λ = 284 nm.**

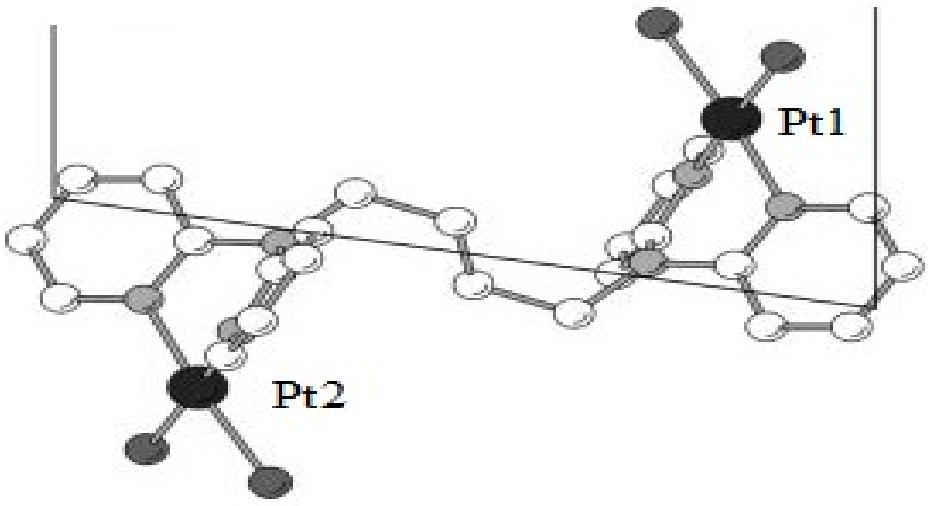

Figure S32: ***Anti*-conformational structure of alkyl complexes with even (-CH_2)n) group.[42] Hydrogen atoms left out for clarity.**

Figure S33: ***Anti- and Syn* conformational structure of alkyl complexes with even and odd (-CH_2)n group**.[61d]

With this variation in structural conformations, different substitution behaviour in the reactivity is expected as observed in this investigation

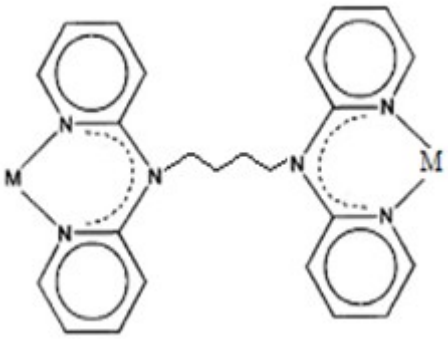

Figure S34: **Proposed conjugated system that stabilizes the metal centre (M)**

The metal atoms are in a conjugation six-membered ring, which makes the electron density to be delocalized into the rings causing deshielding of the alkyl protons. As such the metal alkyl protons are shifted downfield and the ligand protons shifted upfield as revealed in this study.

Figures S4.34 and S4.35 are full spectra of even numbered alkyl chain complexes showing similar substitution behaviour of two separate kinetic steps on the UV-Vis spectrophotometer. On the contrary Figures S4.36 and S4.37 are also full spectra of odd numbered alkyl chain complexes showing similar kinetic behaviour but different from even numbered alkyl chain complexes. Only one kinetic step was observed on the UV-Vis spectrophotometer for these moieties.

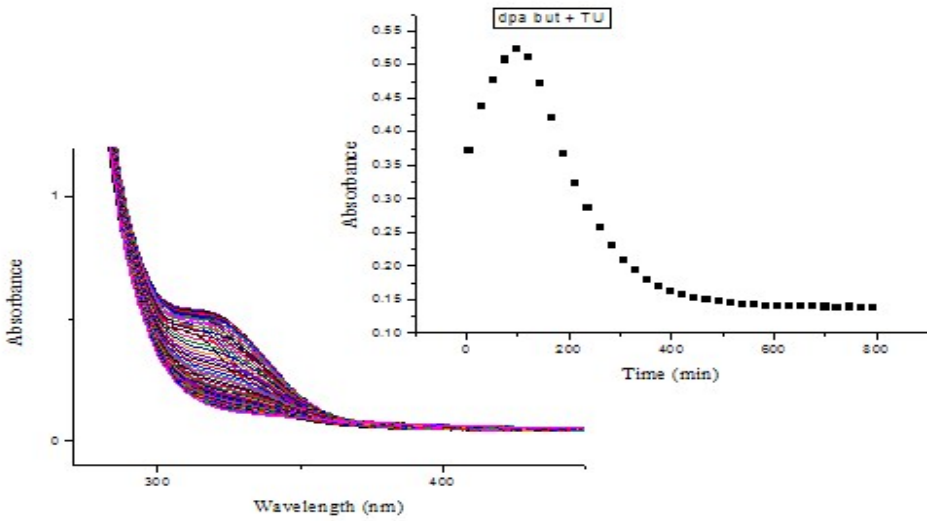

Figure S35: UV/Vis spectral changes observed during the reaction between **PtL4** and **TU**; *inset* is a typical kinetic trace for time dependence of absorbance at 320 nm, T = 298.15 K, pH = 2.0 and I = 0.1 M $NaClO_4$.

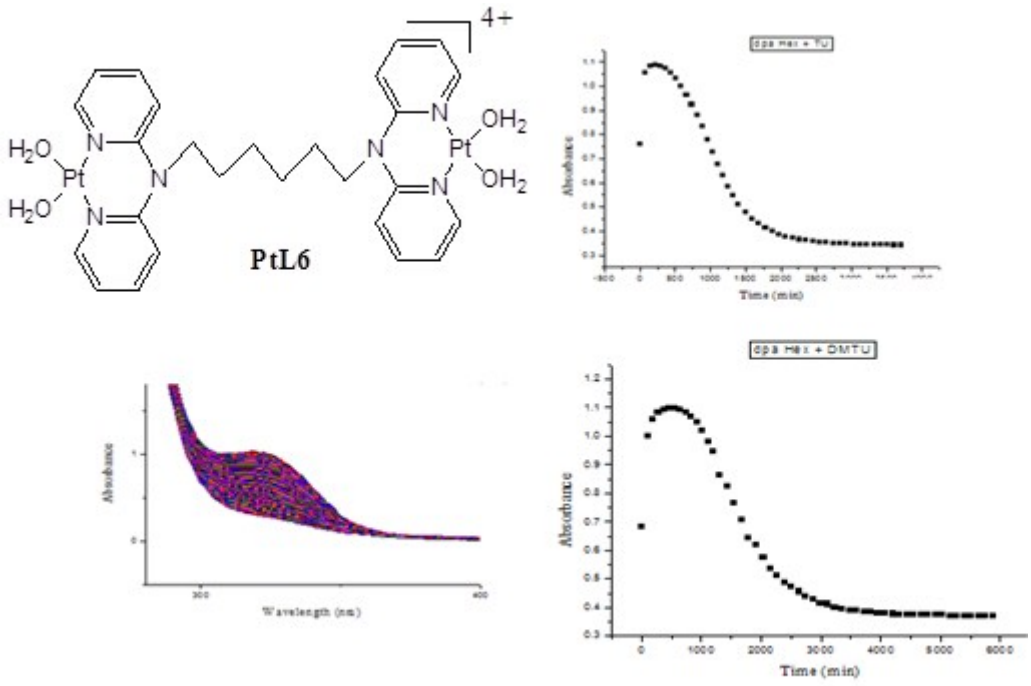

Figure S36: UV/Vis spectral changes observed during the reaction between **PtL6** and **TU** and **DMTU**; *inset* is a typical kinetic trace for time dependence of absorbance at 320 nm, T = 298.15 K, pH = 2.0 and I = 0.1 M $NaClO_4$.

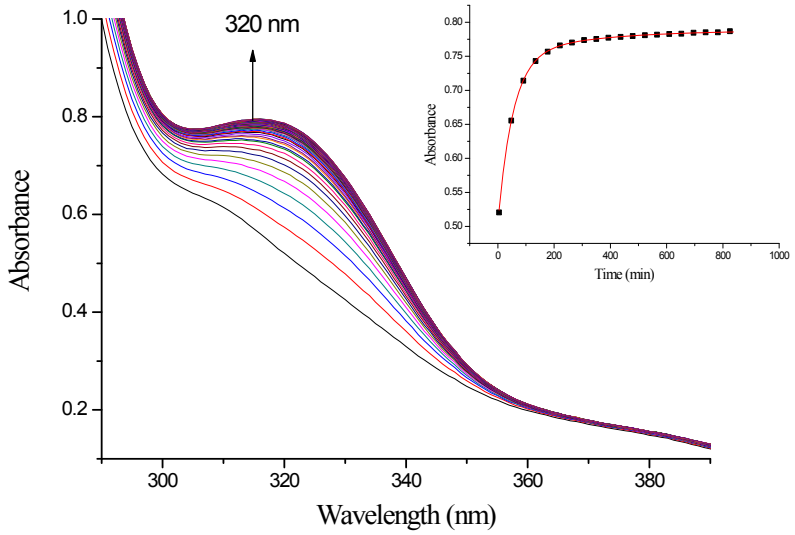

Figure S37: UV/Vis spectral changes observed during the reaction between **PtL3** and **TU**; *inset* is a typical kinetic trace for time dependence of absorbance at 320 nm, T = 298.15 K, pH = 2.0 and I = 0.1 M $NaClO_4$.

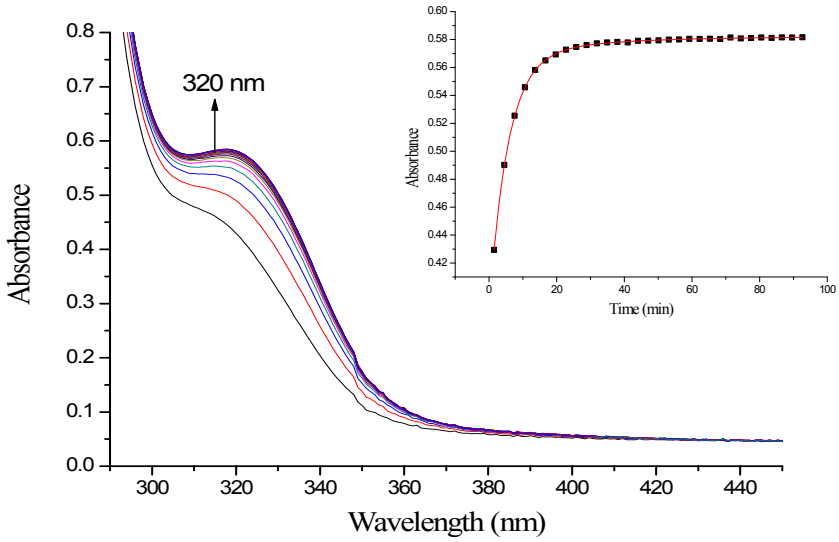

Figure S38: UV/Vis spectral changes observed during the reaction between **PtL5** and **TU**; *inset* is a typical kinetic trace for time dependence of absorbance at 320 nm, T = 298.15 K, pH = 2.0 and I = 0.1 M $NaClO_4$.

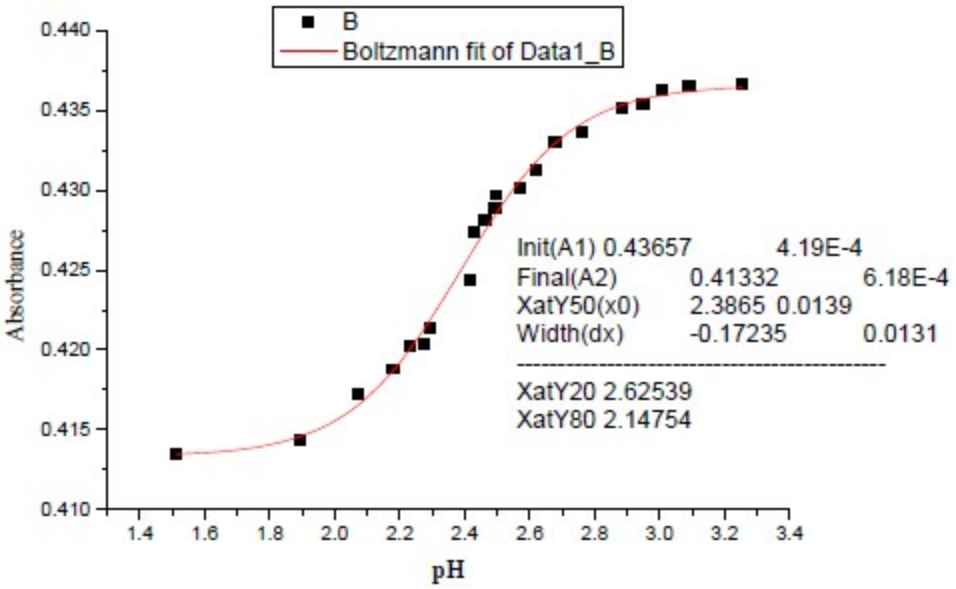

Figure S39: Determination of pK_a values using Boltzmann equation from the sigmoid curve at the inflection point.

Boltzmann Equation: $y = A_2+(A_1 - A_2)/(1 + \exp((x - x_0)/dx)$.

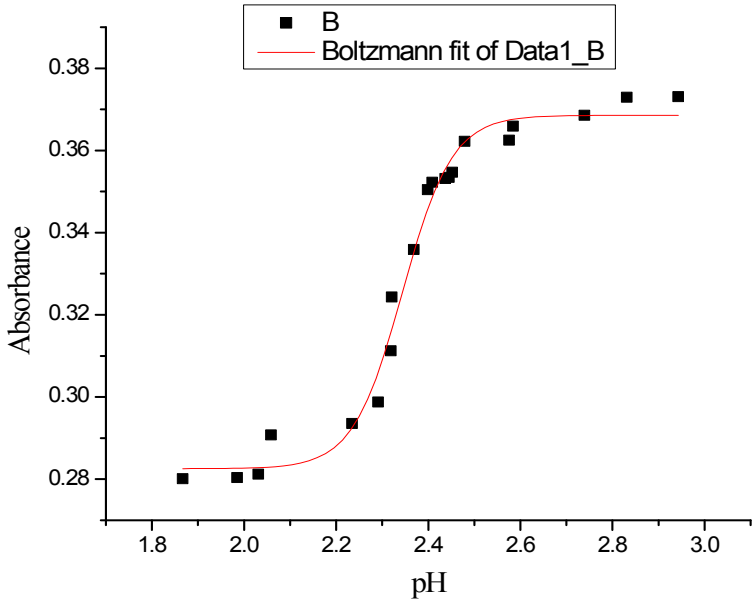

Figure S40: Determination of pK_a values using Boltzmann equation from the sigmoid curve at the inflection point.

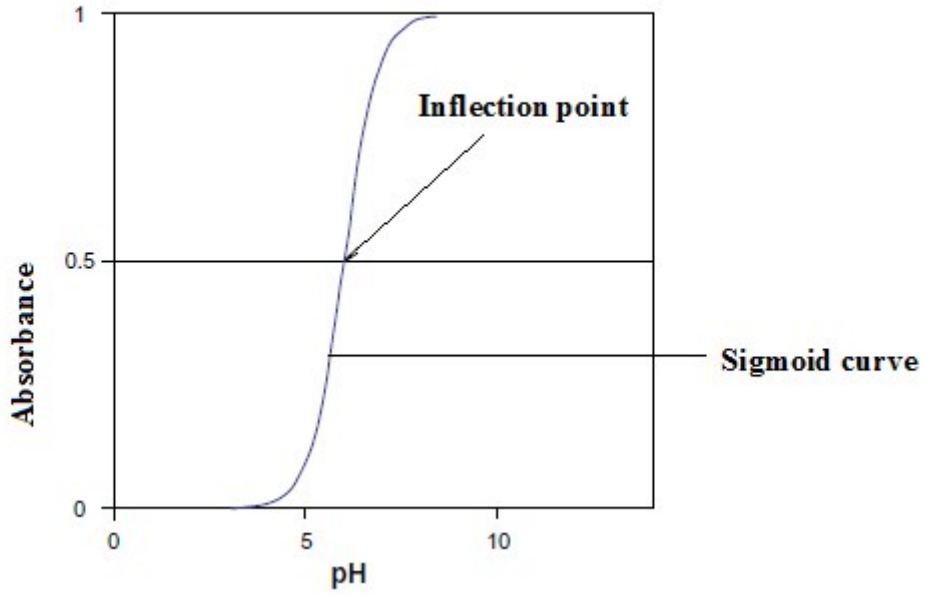

Figure S41: A classic example of a sigmoid curve obtained by plotting absorbance versus pH. The inflection point corresponds to pK_a that were reported.